Original Article

H19/miR-152-3p/TCF4 axis increases chemosensitivity of gastric cancer cells through suppression of epithelial-mesenchymal transition

Xiaodong Jiang, Wenbin Ding, Weiguang Shen, Jie Jin

Department of Interventional Medicine, Nantong First People's Hospital (the Second Affiliated Hospital of Nantong University), Nantong 226001, China

Contributions: (I) Conception and design: X Jiang, J Jin; (II) Administrative support: W Ding, W Shen; (III) Provision of study materials or patients: X Jiang, W Ding, J Jin; (IV) Collection and assembly of data: All authors; (V) Data analysis and interpretation: X Jiang, W Shen, J Jin; (VI) Manuscript writing: All authors; (VII) Final approval of manuscript: All authors.

Correspondence to: Jie Jin. Department of Interventional Medicine, Nantong First People's Hospital (the Second Affiliated Hospital of Nantong University), No. 6 North Road, Haier lane, Nantong 226001, China. Email: jinjiejinj@sina.com.

Background: Adriamycin (ADM) is a drug commonly used for treating gastric cancer (GC). However, chemoresistance presents an obstacle to achieving successful outcomes in patients treated with chemotherapy. This study aimed to explore the effect of long non-coding RNA (lncRNA) H19 on chemoresistance in GC and its potential molecular mechanism.

Methods: The expression of H19 was detected in GC tissues and cell lines. The interaction between miR-152 with H19 and transcription factor 4 (TCF4) was validated by luciferase reporter assay. CCK-8 and flow cytometry were employed to measure cell viability and apoptosis, respectively. The levels of epithelial-mesenchymal transition (EMT) markers (E-cadherin, N-cadherin, Slug, Snail, and Twist) were detected by Western blot assay. A mouse model was established by subcutaneously injecting MGC-803 cells stably transfected with sh-H19 to investigate the effect of H19/miR-152-3p/TCF4 axis on ADM *in vivo*.

Results: *In vitro*, we observed that H19 was overexpressed in GC tissues and cell lines. After knockdown of H19, the IC50 of ADM was decreased and cell apoptosis rates increased in both BGC-823^{ADM} and MGC-803^{ADM} cells. Furthermore, H19 shRNA was found to inhibit epithelial-mesenchymal transition (EMT), and induction of EMT counteracted the inhibitory effect of H19 shRNA on chemoresistance of GC cells. miR-152 was a target of H19, and its expression was downregulated in GC tissues and cell lines. Furthermore, the expression of TCF4 was negatively regulated by miR-152 but positively regulated by H19. *In vivo*, the data indicated that H19 shRNA enhanced the chemosensitivity of GC tumor cells to ADM through sponging miR-152 from TCF4, resulting in the suppression of EMT.

Conclusions: The results of this study elucidated that H19 was overexpressed in GC tissues and cell lines, and knockdown of lncRNA H19 increased the chemosensitivity of GC cells to ADM via sponging miR-152 from TCF4. The H19/miR-152/TCF4 axis may provide a new perspective for treating GC.

Keywords: H19; miR-152-3p; transcription factor 4 (TCF4); chemosensitivity; epithelial-mesenchymal transition

Submitted Feb 26, 2020. Accepted for publication Apr 30, 2020.
doi: 10.21037/tcr-20-1736
View this article at: http://dx.doi.org/10.21037/tcr-20-1736

Introduction

Gastric cancer (GC), a highly common form of malignant tumor, is responsible for approximately 10% of all cancer-related deaths worldwide (1). As a disease that is often asymptomatic early on, the prognosis for GC patients is usually dismal. Although diagnostic techniques and treatments have significantly improved in recent years, GC patients can still expect a low 5-year survival rate of about 20–30% (2). Surgery is currently considered to be the main treatment for GC, while chemotherapy and radiotherapy are the auxiliary means to prevent recurrence and metastasis (3). In patients with late-stage GC for whom the best time for surgery has passed, palliative chemotherapy is the main therapy to increase their prognosis. However, chemoresistance poses an obstacle to achieving successful outcomes for patients who receive chemotherapy (4). Therefore, a deeper understanding of the molecular mechanism of resistance to chemotherapy is crucial to improving the prognosis of GC patients. At present, the research on drug resistance of gastric cancer is not in-depth, which provides us with new ideas.

Epithelial mesenchymal transition (EMT) is a cellular process in which epithelial cells gradually transform into stromal phenotypes (5). There is accumulating evidence to indicate that EMT is an important participant in the chemoresistance of tumor cells. Ying *et al.* showed that, by inhibiting EMT, emodin can effectively reverse the resistance of lung cancer cells to doxorubicin (6). Gaianigo *et al.* elucidated that EMT occurred in the early stage of tumor development and explored its connection with treatment resistance (7). Thus, the chemosensitivity of tumor cells may be increased via the suppression of EMT.

LncRNA-H19 was reported to be an oncogenic lncRNA in several cancers (8). In temozolomide treatment, knockdown of H19 has been identified to sensitize glioma cells to (9). However, the relationship between H19 and chemoresistance in GC cells is yet to be fully established.

In this study, we examined the mRNA levels of H19 in GC tissues and cell lines and explored the role and underlying mechanism of H19 in the chemoresistance to adriamycin (ADM) in GC cells. The data revealed that H19 was overexpressed in GC tissues and cell lines and that the chemosensitivity of GC cells can be increased by inhibiting H19 through the suppression of the EMT via the H19/miR-152-3p/transcription factor 4 (TCF4) axis.

We present the following article in accordance with the ARRIVE reporting checklist (available at http://dx.doi.org/10.21037/tcr-20-1736).

Methods

Clinical specimens

A total of 30 human GC tissues and adjacent normal tissues were obtained from patients who received surgical treatment without radiotherapy and/or chemotherapy at the second affiliated hospital of Nantong university. After surgical resection, all fresh specimens were immediately placed in liquid nitrogen and stored at –80 ℃ until use. This study was approved by the Medical Ethics Committee of the second affiliated hospital of Nantong university.

Cell culture and induction of ADM resistant cells

Human GC cell lines (BGC-823, AGS, MGC-803) and normal gastric epithelium cell lines (GES-1) were obtained from ATCC (Manassas, VA, USA) and cultured in RPMI 1640 medium (Gibco, CA, USA) supplemented with 10% FBS (Gibco, CA, USA) and 1% antibiotics in a humidified incubator (at 37 ℃, 5% CO_2). For the induction of ADM resistant cells (BGC-823 and MGC-803), ADM from 4 ng/mL, the concentration increased by 25%. After 6 months of continuous culture, the subcultures capable of exponential growth at the highest concentration (44 ng/mL) were designated as ADM-resistant cell lines (BGC-823^{ADM} and MGC-803^{ADM}) (10).

Quantitative real-time polymerase chain reaction (qRT-PCR)

Trizol reagent (TaKaRa, Dalian, China) was used to extract total RNA from GC tissues or cells. RNA was reverse transcribed into cDNA using Primescript one-step RT-PCR kit (TaKaRa, Dalian, China). Finally, the expression levels of genes were measured using SYBR Green Master Mix (Life Technologies) with pre-denaturation at 93 ℃ for 5 min, 35 cycles of denaturation at 95 ℃ for 40 sec, then hybridization at 55 ℃ for 60 sec, and followed by a extend at 72 ℃ for 1 min. The levels were calculated via the $2^{-\Delta\Delta Ct}$ mean. GAPDH and U6 served as the controls. The primers used are shown as follows: H19 F: ACCACTGCACTACCTGACTC, R: CCGCAGGGGGTGGCCATGAA; MiR-152-3p F: 5'-GCAGTCAGTGCATGACAGA-3', R: 5'-GTCCAGTTTTTTTTTTTTTTTCCAAG-3'; TCF4 F: 5'-GATCCGTTGGGGAGGTAGG-3', R: 5'-TGGAGGGCTCTTTAAGGGG-3'; GAPDH F: 5'-CTGGGCTACACTGAGCACC-3',

R: 5'-AAGTGGTCGTTGAGGGCAATG-3'; U6 F: 5'-CTCGCTTCGGCAGCACA-3', R: 5'-ACGCTTCACGAATTTGCGT-3'.

Cell transfection

shRNA against H19 (H19 shRNA), miR-152 mimic, miR-152 inhibitor, pcDNA3.0-TCF4 (TCF4/pcDNA3.0), and the corresponding negative controls (H19 scramble, mimic NC, inhibitor NC, and pcDNA3.0 vector) were synthesized from Santa Cruz (CA, USA). The sequences were as follows: H19 shRNA: 5'-GCGGGUCUGUUUCUUUACUUU-3'; H19 scramble: 5'-GACCAGCTGTCTAGGACTGACTT-3'; miR-152 mimic: 5'-UCAGUGCAUGACAGAACUUGG-3'; mimic NC: 5'-UUCUCCGAACGUGUCACGUTT-3'; miR-152 inhibitor: 5'-UGUUAAGCUGUCUCUGGCUUG-3'; inhibitor NC: 5'-UUUCCAAGGAAAGAGACAGCU-3'; TCF4/pcDNA3.0: 5'-CCGGGCTGAGTGATTTACTGGATTTCTCGAGA-3'; pcDNA3.0 Vector: 5'-CGAAAAAGCTGAGTGATTTACTGGATTTCT-3'. GC cells were inoculated into 6-well plates at a density of 1×10^6 and cultured to 70% confluence. Lipofectamine 2000 (Invitrogen, USA) was then used to transfect molecular products into the cells.

Cell viability assay

Transfected BGC-823^{ADM} or MGC-803^{ADM} cells were seeded in 96-well plates at a concentration of 5×10^4 cells/well. After 24 h of incubation with ADM (0–8 μM), 20 μL of MTT solution (5 mg/mL, Sigma, MO, USA) was added to the medium, and the cells were incubated at 37 ℃ for a further 4 h. Next, 150 μL of dimethy sulfoxide (DMSO, Sigma, MO, USA) was used in place of the entire supernatant, and the formalazine crystals were dissolved at 37 ℃ for 30 min. Finally, the absorbance at 490 nm of each well was measured with a microplate reader (Bio-Rad).

Cell apoptosis analysis

Cells with a number of 2×10^5 were cleaned twice with PBS and then resuspended in 500 μL Annexin-binding buffer. Next, 5 μL Anexin v-FIFC and 10 μL PI were added to the suspension and reacted at room temperature for 10 min. After incubation with DAPI staining for 20 min in the dark, the rate of cell apoptosis was analyzed by flow cytometry (BD Biosciences, San Jose, California, USA).

Western blot analysis

Cells were lysed with RIPA lysis buffer (Beyotime, Shanghai, China), and a bicinchoninic acid Protein Assay Kit was used to measure protein concentrations (CoWin Biotechnology, Beijing, China). The protein lysate (30 μg) in each sample was isolated with a 10% SDS-PAGE gel and transferred to a PVDF membrane (Bio-Rad, CA, USA). The membranes were blocked with 5% low-fat milk for 1 h at 37 ℃, before incubation with primary antibody (1:1,000; anti-Twist, anti-Snail, anti-Slug, anti-TCF4, anti-E-cadherin, anti-N-cadherin, and anti-GAPDH antibodies, CST) overnight at 4 ℃. The following day, the membranes were incubated with the corresponding secondary antibodies (1:5,000, CST) for 1 h at room temperature, respectively. The imprinted membranes were visualized using an ECL system (Bio-Rad Laboratories).

Luciferase reporter assay

H19 wild-type (wt-H19) and TCF4 wild-type (wt-TCF4) luciferase vectors were constructed including mutated binding sites (mut-H19 and mut-TCF4, respectively). Cells were promptly co-transfected with wt or mut and miR-152-3p mimics using Lipofectamine 2000 (Invitrogen, USA) according to the manufacturer's instructions. The luciferase activity buffer (Promega, WI, USA) was added to the 24-well plate containing the transfected cells, followed by placed on a shaker to lyse them sufficiently. Finally, luciferase activity was detected using a dual-luciferase reporter system (Promega, WI, USA).

In vivo animal study

Male BALB/c 4-week-old nude mice were obtained from the laboratory animal center of Nantong university. All operations were in accordance with the National Institute of Health Guide for the Care and Use of Laboratory Animals (8th edition, NIH Publications, revised 2011) and were approved by the medical ethics committee of the Second Affiliated Hospital of Nantong University. The mice were housed in a standard environment (at 23±1 ℃, relative humidity 60%±10%, and a 12-h light/dark cycle) with free access to water and food. The mice were divided at random into groups (n=5): the control group mice were subcutaneously injected with MGC-803^{ADM} cells suspension (1×10^6/mL) into the flank area; the ADM-treated group mice were injected with MGC-803^{ADM} cells and treated with

ADM (10 mg/kg); and the ADM + H19 shRNA group mice were injected with H19 shRNA-transfected MGC-803^{ADM} cells and treated with ADM (10 mg/kg). Tumor volume and the body weight in mice were measured every 5 days after injection. The mice were sacrificed at 30 days after injection and tumors were collected for follow-up study.

TdT-mediated dUTP nick-end labeling (TUNEL) assay

Briefly, the tissue sections were incubated in 3% H_2O_2, and then mixed with the TUNEL reaction mixture (Beyotime, Jiangsu, China), in line with the manufacturer's instructions. Positive cells were visualized using a DAB kit (Beyotime, Jiangsu, China) and counterstained using Hematoxylin. For positive cell count, six visual fields were selected at random under a light microscope (Olympus Corporation, Tokyo, Japan).

Statistical analysis

Data in our present study were presented as mean ± standard deviation (SD) and statistical analysis was conducted using SPSS 20.0 software. Differences between two groups were analyzed with Student's *t*-test (unpaired, two tailed) and differences among multiple groups were analyzed with one-way analysis of variance (ANOVA). Statistical significance was considered to exist when P<0.05.

Results

H19 is upregulated in GC tissues and cells

Our data revealed that the mRNA level of H19 was upregulated in GC tissues compared with normal tissues (*Figure 1A*, P<0.001). The expression of H19 was also higher in GC cell lines (BGC-823, AGS and MGC-803) than in GES-1 (*Figure 1B*, P<0.01). These results indicated that H19 was overexpressed in GC tissues and cells.

H19 shRNA increases chemosensitivity of GC cells to ADM

H19 shRNA transfection significantly decreased relative expression of H19 in ADM-resistant GC cell lines (*Figure 1C*, P<0.01). Moreover, the IC_{50} values of ADM were approximately 1.2 and 3.3 μM in the ADM + H19 shRNA and ADM + H19 scramble groups of BGC-823^{ADM} cells, respectively. Simultaneously, the IC_{50} values of ADM were about 0.9 and 3.2 μM in the ADM + H19 shRNA and ADM + H19 scramble groups of MGC-803^{ADM} cells, respectively. These results suggested that knockdown of H19 increased the sensibility of ADM-resistant GC cells to ADM (*Figure 1D,E,F,G,H,I,J,2A,B,C,D,E*, P<0.05). MGC-803^{ADM} cells were chosen for the subsequent experiments. We observed that the cell apoptosis rate of ADM-resistant cells was not influenced remarkably by ADM treatment. However, knockdown of H19 increased the cell apoptosis rate of MGC-803^{ADM} cells compared with the H19 scramble group treated with ADM (*Figure 2F*, P<0.01). Consequently, our results suggested that knockdown of H19 decreased the chemoresistance of GC cells to ADM.

H19 shRNA increases the chemosensitivity of GC cells by inhibiting EMT

Compared with the H19 scramble group, we found that H19 shRNA increased E-cadherin (epithelial marker) but decreased N-cadherin (mesenchymal marker) in MGC-803^{ADM} cells. To induce EMT, we specifically employed TGF-β1 in this study. As shown in *Figure 1G*, TGF-β1 treatment diminished the protein level of E-cadherin while elevating the level of N-cadherin in H19 shRNA-transfected MGC-803^{ADM} cells. In addition, H19 shRNA decreased relative expression of Slug, Snail and Twist while TGF-β1 treatment significantly weakened the effect of H19 shRNA (*Figure 1H*). Furthermore, the IC_{50} values of ADM were 0.9 and 3.2 μM in the H19 shRNA and H19 shRNA+ TGF-β1 groups, respectively, which indicated that the sensitivity of ADM-resistant GC cells to ADM was reduced when EMT was activated by TGF-β1 (*Figure 1I*, P<0.05). TGF-β1 treatment also weakened the cell apoptosis rate (*Figure 1J*, P<0.05). In summary, our data elucidated that TGF-β1-induced EMT attenuated the inhibitory effect of H19 on the chemoresistance of GC cells to ADM.

miR-152-3p is a target of H19

miR-152 was identified as a predicted target of H19 (*Figure 2A*), and the mRNA levels of miR-152 were downregulated in GC tumor tissues and cell lines (*Figure 2B,C*, P<0.05, P<0.01). MGC-803^{ADM} cells were transfected with miR-152 mimic or inhibitor, and miR-152 was successfully transfected, as shown in *Figure 2D* (P<0.05, P<0.01). Furthermore, miR-152 expression was higher in the H19 shRNA group than in the H19 scramble group, with miR-152 inhibitor significantly offsetting this increase; this indicated that the expression of miR-152 was negatively

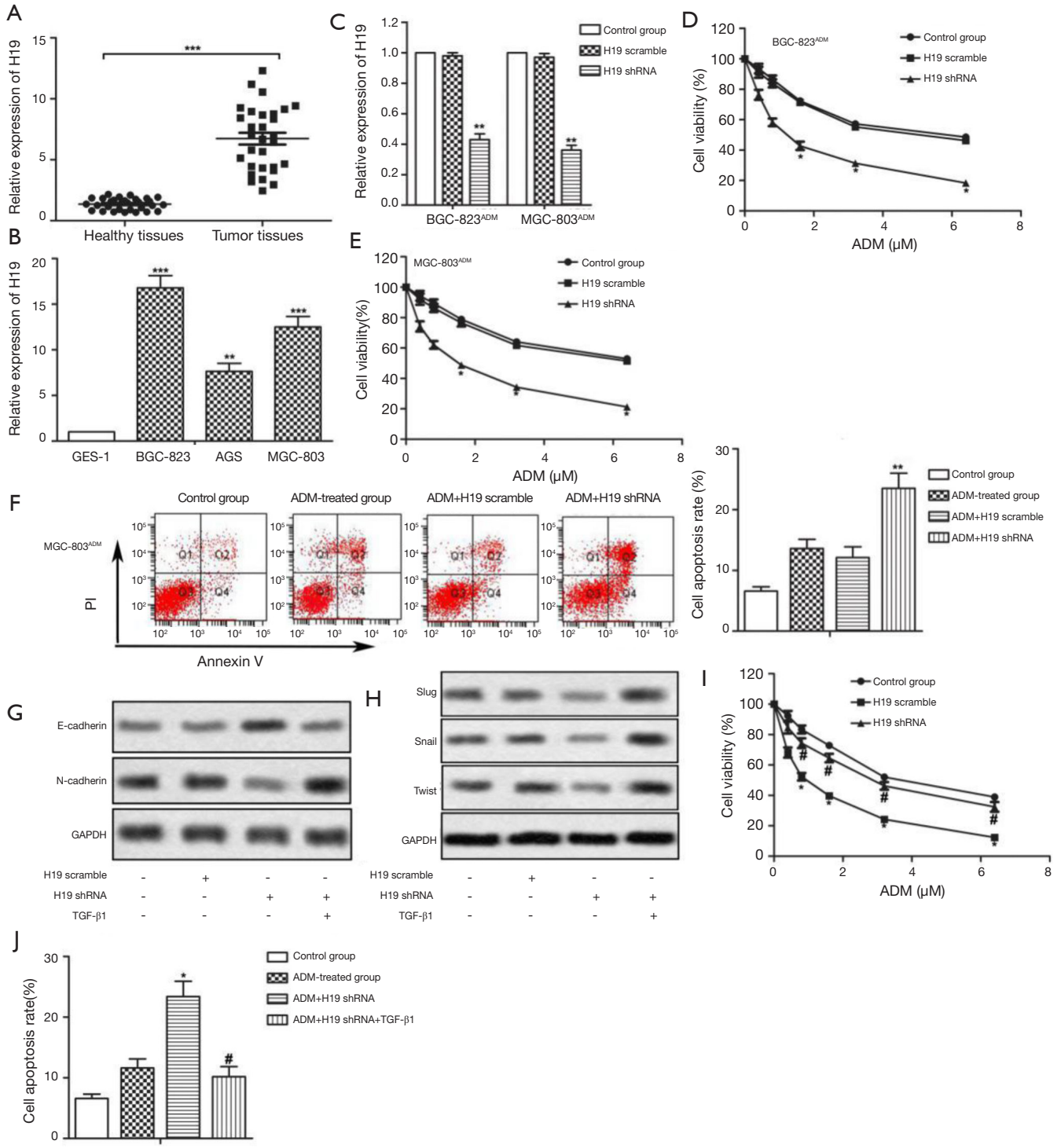

Figure 1 H19 shRNA increases the chemosensitivity of GC cells by inhibiting EMT. (A) The mRNA levels of H19 in healthy and GC tissues were detected by qRT-PCR. ***, P<0.001 *vs.* healthy tissues. (B) The expression of H19 in GES-1 and GC cell lines was detected by qRT-PCR. **, P<0.01 and ***, P<0.001 *vs.* healthy tissues or GES-1, respectively. (C) Relative mRNA levels of H19 were detected by qRT-PCR. **, P<0.01 *vs.* the H19 scramble group. (D,E) Cell viability was detected by MTT assay. *, P<0.05 *vs.* the control group. (F) Cell apoptosis was detected by flow cytometry. **, P<0.01 *vs.* the ADM + H19 scramble group. (G,H) Relative expressions of E-cadherin, N-cadherin, Slug, Snail, and Twist were detected by Western blotting. (I) Cell viability was detected by MTT assay. *, P<0.05 *vs.* the control group; #, P<0.05 *vs.* the H19 shRNA group. (J) Cell apoptosis was detected by flow cytometry. *, P<0.05 *vs.* the ADM + H19 scramble group; #, P<0.05 *vs.* the ADM + H19 shRNA group. Data were represented as the mean ± SD.

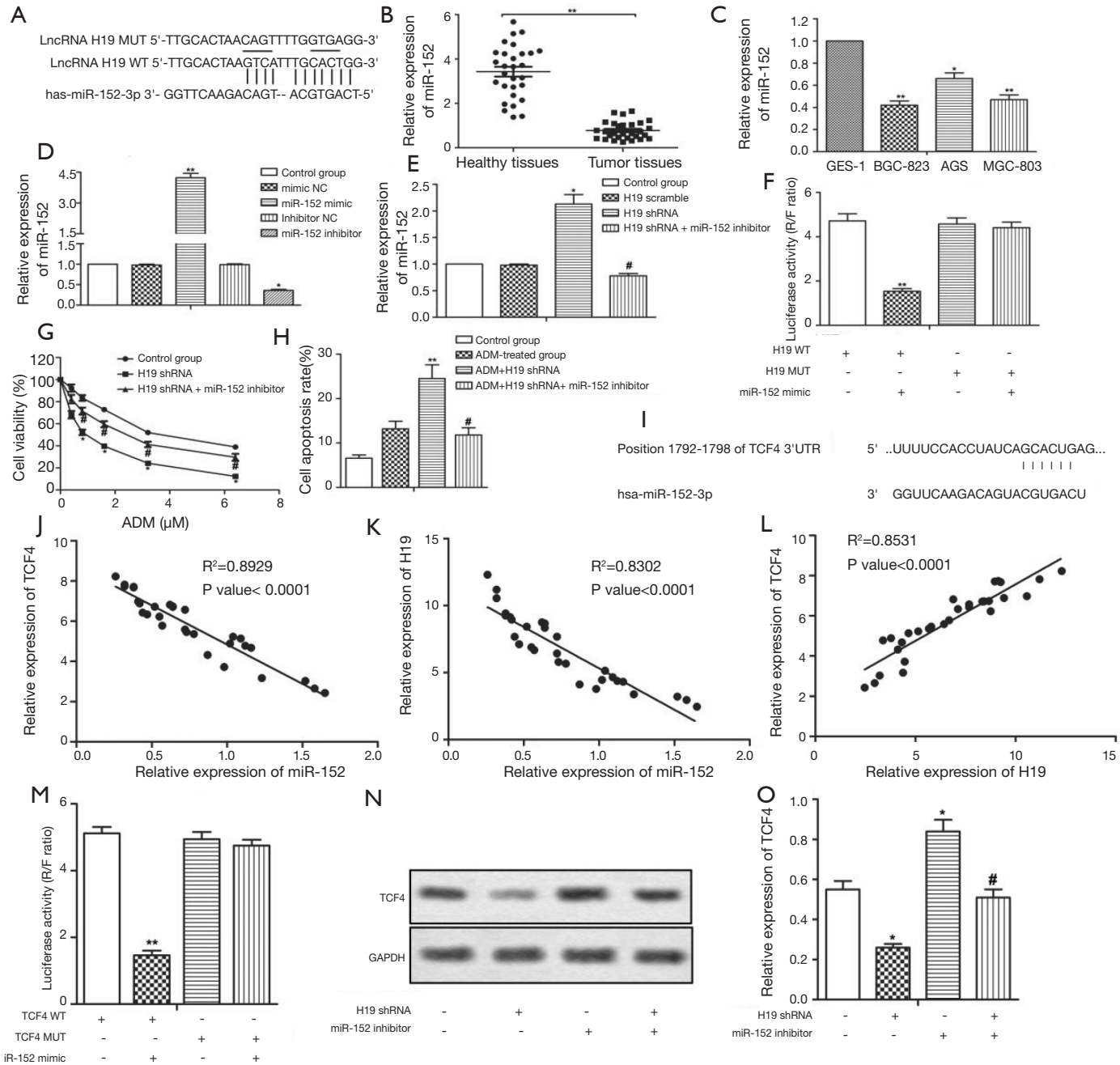

Figure 2 H19 shRNA enhances the chemosensitivity of GC cells via the MiR-152-3p/TCF4 axis. (A) The target relationship between miR-152 and H19 mRNA was analyzed by bioinformatics analysis. (B) The mRNA levels of miR-152 in healthy tissues and GC tissues were measured by qRT-PCR. **, P<0.01 *vs*. healthy tissues. (C) The mRNA levels of miR-152 in GES-1and GC cell lines were measured by qRT-PCR. *, P<0.05 and **, P<0.01 *vs*. GES-1. (D,E) The relative mRNA levels of miR-152 were measured by qRT-PCR. *, P<0.05 and **, P<0.01 *vs*. the control group; #, P<0.05 *vs*. the ADM + H19 shRNA group. (F) The interaction between H19 and miR-152 was checked by luciferase reporter assay. **, P<0.01 *vs*. H19 WT group. (G) Cell viability was detected by MTT assay. *, P<0.05 *vs*. the control group; #, P<0.05 *vs*. the H19 shRNA group. (H) Cell apoptosis was detected by flow cytometry. **, P<0.01 *vs*. the control group; #, P<0.05 *vs*. the ADM + H19 shRNA group. (I) The target relationship between miR-152 and TCF4 was analyzed by bioinformatics analysis. (J,K,L) The mutual relationship among H19, miR-152, and TCF4 was measured through qRT-PCR. (M) The interaction between TCF4 and miR-152 was checked by luciferase reporter assay. **, P<0.01 *vs*. TCF4 WT group. (N,O) The expression of TCF4 was measured by Western blotting. *, P<0.05 *vs*. the control group; #, P<0.05 *vs*. the miR-152 inhibitor group. Data were represented as the mean ± SD.

regulated by H19 (*Figure 2E*, P<0.05, P<0.05). Luciferase reporter assay was applied to further confirm the target relationship between miR-152 and H19. As expected, luciferase activity in MGC-803^{ADM} cells was significantly decreased by co-transfection with wt-H19 and miR-152 mimic, but co-transfection with mut-H19 and miR-152 mimic rescued this change (*Figure 2F*, P<0.01). The IC_{50} values of ADM were 0.9 and 2.9 μM in the H19 shRNA group and H19 shRNA + miR-152 inhibitor group, respectively, which demonstrated that downregulation of miR-152 could counteract the inhibitory effect of H19 shRNA on the chemoresistance of GC cells to ADM (*Figure 2G*, P<0.05). Moreover, the cell apoptosis rate was suppressed by miR-152 inhibitor in this group compared with the ADM + H19 shRNA group (*Figure 2H*, P<0.01, P<0.05). Taken together, these data showed that miR-152 was a direct target of H19 and was negatively regulated by H19. Inhibition of miR-152 weakened the inhibitory effect of H19 shRNA on the chemoresistance of GC cells to ADM.

TCF4 expression is regulated by miR-152 and H19 in GC cells

Bioinformatics analysis revealed TCF4 to be a potential target of miR-152 (*Figure 2I*). The expressions of TCF4, H19, and miR-152 were then analyzed, and it was observed that miR-152 was negatively correlated with TCF4 (*Figure 2J*, P<0.0001) or H19 (*Figure 2K*, P<0.0001), but TCF4 was positively correlated with H19 (*Figure 2L*, P<0.0001). Luciferase reporter assay further demonstrated that TCF4 was a direct target of miR-152 (*Figure 2M*, P<0.01). In addition, the mRNA level of TCF4 was downregulated in the H19 shRNA group but upregulated in the miR-152 inhibitor group (*Figure 2N,O*, P<0.05). All of these results indicated that TCF4 was positively regulated by H19 and negatively regulated by miR-152.

Overexpressed TCF4 decreases the chemosensitivity of GC cells to ADM through inducing EMT

MGC-803^{ADM} cells were transfected with pcDNA3.0-TCF4 or pcDNA3.0 vector (*Figure 3A,B*, P<0.01). The protein level of E-cadherin was significantly downregulated by TCF4 overexpression, while the level of N-cadherin was upregulated (*Figure 3C,D*, P<0.05). The IC_{50} values of ADM were approximately 3.2 and 5.7 μM in the pcDNA3.0 vector group and the TCF4/pcDNA3.0 group, respectively (*Figure 3E*). Similarly, overexpressed TCF4 also suppressed cell apoptosis in ADM-resistant GC cells under the treatment of ADM although the difference was not obvious (*Figure 3F*). These results determined that TCF4 overexpression decreased the chemosensitivity of GC cells to ADM by inducing EMT.

H19 shRNA enhanced the chemosensitivity of GC tumor cells to ADM in vivo

Tumor volume and the body weight in mice were not significantly affected by ADM treatment. Compared with the ADM treated group, H19 shRNA transfection suppressed tumorigenesis and maintained body weight (*Figure 4A,B*, P<0.05). TUNEL assay revealed the apoptosis index to be significantly increased by H19 shRNA compared to treatment with ADM (*Figure 4C,D*, P<0.05). The mRNA level of miR-152 was also increased, while the protein level of TCF4 was decreased in the ADM + H19 shRNA group compared with the group treated with ADM (*Figure 4E,F,G*, P<0.05). Furthermore, E-cadherin expression was increased and N-cadherin expression was decreased in the ADM + H19 shRNA group compared with the ADM-treated group (*Figure 4H,I,J*, P<0.05). Our data revealed that H19 shRNA enhanced the chemosensitivity of GC tumor cells to ADM *in vivo* through sponging miR-152 from TCF4, resulting in the suppression of EMT.

Discussion

GC metastasis and recurrence can be prevented by chemotherapy. However, the clinical application of chemotherapy in GC has been severely restricted by chemoresistance. In our present study, we confirmed that H19 shRNA enhanced the chemosensitivity of ADM-resistant GC cells to ADM, both *in vitro* and *in vivo*, through sponging miR-152 from TCF4, resulting in the suppression of EMT.

In recently published studies, lncRNA H19 was found to be markedly elevated in multiple tumor types including breast, ovarian, and bladder cancer, in which it functioned as an oncogene (11-13). Previous reports showed that H19 was involved in the chemoresistance of tumor cells. Jiang, for example, elucidated that H19 knockdown sensitized glioma cells to temozolomide therapy (9). Meanwhile, H19 has been found to induce paclitaxel chemoresistance in breast cancer by silencing BIK (14). Similarly, in the present study, H19 was also observed to be overexpressed in GC. Consequently, H19 shRNA led to decreased IC_{50} values

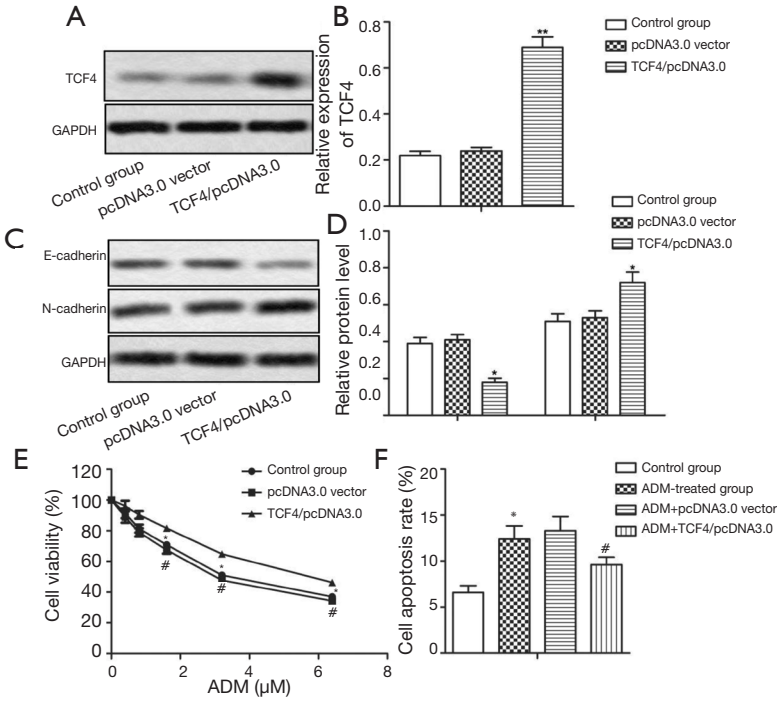

Figure 3 Overexpression of TCF4 decreases the chemosensitivity of GC cells to ADM by inducing EMT. MGC-803^{ADM} cells transfected with pcDNA 3.0 vector or TCF4/pcDNA3.0 received ADM treatment with untreated cells as a control. (A,B,C,D) The relative expressions of TCF4, E-cadherin, and N-cadherin were measured by Western blotting. *, P<0.05, **, P<0.05 *vs*. the control group. (E) Cell viability was measured by MTT assay. *, P<0.05, #, P<0.05 *vs*. the control group. (F) Cell apoptosis was measured by flow cytometry. *, P<0.05 *vs*. the control group; #, P<0.05 *vs*. the ADM + pcDNA3.0 vector group. Data were represented as the mean ± SD.

of ADM and increased apoptosis in both BGC-823^{ADM} and MGC-803^{ADM} cells, which suggests that H19 shRNA could increase the chemosensitivity of GC cells to ADM. In our study, we revealed that H19 shRNA inhibited EMT. TGF-β1 is well-known to induce EMT (15). TGF-β1 treatment abolished the changes made by H19 shRNA, indicating that chemosensitivity was increased by H19 shRNA through its suppression of EMT.

H19 has been reported to regulate the inhibition of miRNA targets at the post-transcriptional level. Su reported that H19, as a competing endogenous RNA, regulated the expression of AQP3 by sponging miR-874 in the intestinal barrier (16). H19 was also reported to contribute to cell proliferation in gallbladder cancer through modulation of AKT expression by sponging miR-194-5p (17). In present study, we uncovered a direct binding relationship between miR-152 and H19. Meanwhile, we observed that miR-152 was downregulated in GC, and its expression was negatively regulated by H19. Moreover, compared with the ADM+H19-shRNA group, co-transfection of H19shRNA and miR-152 inhibitors elevated the IC50 value of ADM and reduced the apoptosis rate, suggesting that the knockout of miR-152 abolished the inhibition of H19-shRNA in cellular ADM chemoresistance. Overall, these data indicated that H19 acted as an miR-152 sponge to regulate the chemoresistance of GC cells, which was consistent with our hypothesis.

TCF4 is a basic helix-loop-helix transcription factor, which is reported to play an important role during EMT (18). Our present study revealed that the mRNA level of TCF4 was negatively regulated by miR-152, and positively regulated by H19. Consistently, TCF4 overexpression induced EMT by decreasing the protein expression of E-cadherin while increasing N-cadherin. Additionally, TCF4 overexpression also decreased GC cell chemosensitivity to ADM. In all, our *in vitro* experiments indicated that H19 shRNA increased the chemosensitivity of GC cells to ADM via derepression of miR-152 from TCF4.

Animal experiments were also employed to explore the effect of H19 *in vivo*. Previous study has indicated that

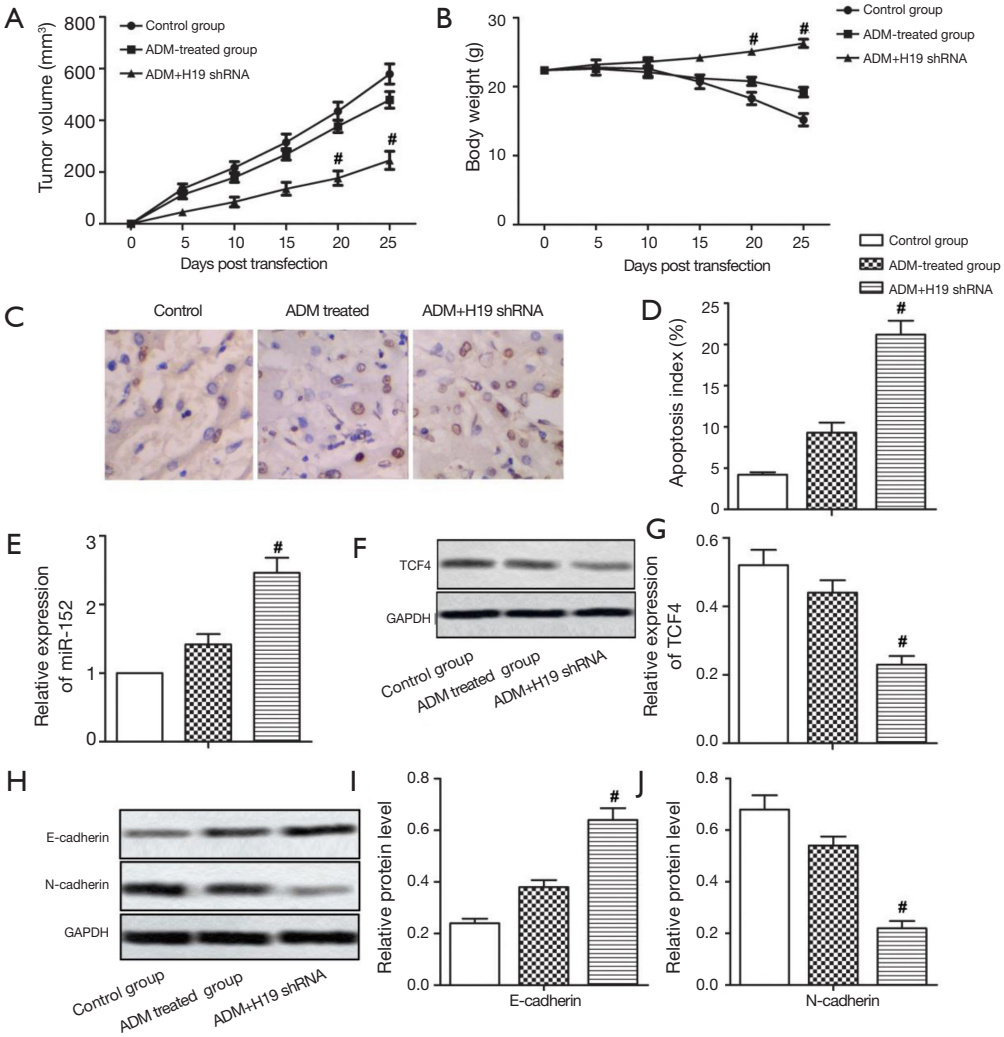

Figure 4 H19 shRNA enhances the chemosensitivity of GC tumor cells to ADM *in vivo*. MGC-803^{ADM} cells (with and without H19 shRNA transfection) were injected into nude mice and treated with ADM. (A,B) The tumor volume and body weight of the mice were detected every 5 days. #, P<0.05 *vs*. the ADM-treated group. (C,D) Apoptosis index was measured by TUNEL staining, images were magnified at 400×. #, P<0.05 *vs*. the ADM-treated group. (E) The mRNA level of miR-152 was measured by qRT-PCR. #, P<0.05 *vs*. the ADM-treated group. (F,G,H,I,J) The protein level of TCF4 was measured by Western blotting. #, P<0.05 *vs*. the ADM-treated group. Data were represented as the mean ± SD.

H19 shRNA strongly reduces tumor growth and tumor volume in colon cancer (19). Similarly, we also found that H19 shRNA reduced tumor growth and tumor volume in GC while maintaining the body weight of the mice under the treatment of ADM. In addition, H19 shRNA increased the apoptosis index and suppressed EMT. Particularly, the mRNA and protein levels of miR-152 were increased and the levels of TCF4 were decreased by H19 shRNA, indicating that the H19-miR-152-3p-TCF4 axis suppressed GC tumor progression by inhibiting EMT when treated with ADM.

In conclusion, our study demonstrated that H19 was aberrantly upregulated in GC tissues and cell lines, TCF4 was positively regulated by H19 and negatively regulated by miR-152. Knockdown of H19 increased the chemosensitivity of GC cells to ADM via sponging miR-152 from TCF4, overexpressed TCF4 abrogated the effect of H19 on the chemosensitivity of GC cells through

inducing EMT. The H19/miR-152/TCF4 axis may be a new prospect in the treatment of GC.

Acknowledgments

Funding: None.

Footnote

Reporting Checklist: The authors have completed the ARRVIE reporting checklist. Available at http://dx.doi.org/10.21037/tcr-20-1736

Data Sharing Statement: Available at http://dx.doi.org/10.21037/tcr-20-1736

Conflicts of Interest: All authors have completed the ICMJE uniform disclosure form (available at http://dx.doi.org/10.21037/tcr-20-1736). The authors have no conflicts of interest to declare.

Ethical Statement: The authors are accountable for all aspects of the work in ensuring that questions related to the accuracy or integrity of any part of the work are appropriately investigated and resolved. This study was approved by the Medical Ethics Committee of the Second Affiliated Hospital of Nantong University (approval ID: SYXK-Su-20200017).

References

1. Ferlay J, Shin HR, Bray F, et al. Estimates of worldwide burden of cancer in 2008: GLOBOCAN 2008. Int J Cancer 2010;127:2893-917.
2. Sun Z, Jia J, Du F, et al. Clinical significance of serum tumor markers for advanced gastric cancer with the first-line chemotherapy. Transl Cancer Res 2019;8:2680-90.
3. Wu W, Ding H, Cao J, et al. FBXL5 inhibits metastasis of gastric cancer through suppressing Snail1. Cell Physiol Biochem 2015;35:1764-72.
4. Cunquero-Tomás AJ, Ortiz-Salvador JM, Iranzo V, et al. Sweet syndrome as the leading symptom in the diagnosis of gastric cancer. Chin Clin Oncol 2018;7:11.
5. Thiery JP, Acloque H, Huang RY, et al. Epithelial-mesenchymal transitions in development and disease. Cell 2009;139:871-90.
6. Ying Y, Qingwu L, Mingming X, et al. Emodin: One Main Ingredient of Shufeng Jiedu Capsule Reverses Chemoresistance of Lung Cancer Cells Through Inhibition of EMT. Cell Physiol Biochem 2017;42:1063-72.
7. Gaianigo N, Melisi D, Carbone C. EMT and Treatment Resistance in Pancreatic Cancer. Cancers (Basel) 2017. doi: 10.3390/cancers9090122.
8. Matouk IJ, DeGroot N, Mezan S, et al. The H19 non-coding RNA is essential for human tumor growth. PLoS One 2007;2:e845.
9. Jiang P, Wang P, Sun X, et al. Knockdown of long noncoding RNA H19 sensitizes human glioma cells to temozolomide therapy. Onco Targets Ther 2016;9:3501-9.
10. Du MD, He KY, Qin G, et al. Adriamycin resistance-associated prohibitin gene inhibits proliferation of human osteosarcoma MG63 cells by interacting with oncogenes and tumor suppressor genes. Oncol Lett 2016;12:1994-2000.
11. Vennin C, Spruyt N, Dahmani F, et al. H19 non coding RNA-derived miR-675 enhances tumorigenesis and metastasis of breast cancer cells by downregulating c-Cbl and Cbl-b. Oncotarget 2015;6:29209-23.
12. Medrzycki M, Zhang Y, Zhang W, et al. Histone h1.3 suppresses h19 noncoding RNA expression and cell growth of ovarian cancer cells. Cancer Res 2014;74:6463-73.
13. Luo M, Li Z, Wang W, et al. Long non-coding RNA H19 increases bladder cancer metastasis by associating with EZH2 and inhibiting E-cadherin expression. Cancer Lett 2013;333:213-21.
14. Si X, Zang R, Zhang E, et al. LncRNA H19 confers chemoresistance in ERalpha-positive breast cancer through epigenetic silencing of the pro-apoptotic gene BIK. Oncotarget 2016;7:81452-62.
15. Moustakas A, Heldin CH. Mechanisms of TGFbeta-Induced Epithelial-Mesenchymal Transition. J Clin Med 2016. doi: 10.3390/jcm5070063.
16. Su Z, Zhi X, Zhang Q, et al. LncRNA H19 functions as a

competing endogenous RNA to regulate AQP3 expression by sponging miR-874 in the intestinal barrier. FEBS Lett 2016;590:1354-64.
17. Wang SH, Wu XC, Zhang MD, et al. Long noncoding RNA H19 contributes to gallbladder cancer cell proliferation by modulated miR-194-5p targeting AKT2. Tumour Biol 2016;37:9721-30.
18. Forrest MP, Waite AJ, Martin-Rendon E, et al. Knockdown of human TCF4 affects multiple signaling pathways involved in cell survival, epithelial to mesenchymal transition and neuronal differentiation. PLoS One 2013;8:e73169.
19. Yang Q, Wang X, Tang C, et al. H19 promotes the migration and invasion of colon cancer by sponging miR-138 to upregulate the expression of HMGA1. Int J Oncol 2017;50:1801-9.

Cite this article as: Jiang X, Ding W, Shen W, Jin J. H19/miR-152-3p/TCF4 axis increases chemosensitivity of gastric cancer cells through suppression of epithelial-mesenchymal transition. Transl Cancer Res 2020;9(6):3915-3925. doi: 10.21037/tcr-20-1736

